processes

MDPI

Article

Design, Construction, and Characterization of a Solar Photovoltaic Hybrid Heat Exchanger Prototype

Sandro Guadalupe Perez Grajales [1], Angel Horacio Hernández [2], David Juárez-Romero [1], Guadalupe Lopez Lopez [3] and Gustavo Urquiza-Beltran [1,*]

1 Centro de Investigación en Ingeniería y Ciencias Aplicadas (CIICAp) de la Universidad Autónoma del Estado de Morelos, Av. Universidad No. 1001, Col Chamilpa, Cuernavaca C.P. 62209, Morelos, Mexico; sandro.perez@uaem.mx (S.G.P.G.); djuarezr7@gmail.com (D.J.-R.)
2 División de Ingeniería Mecánica, Mecatrónica e Industrial, Tecnológico de Estudios Superiores de Ecatepec (TESE), Av. Tecnológico s/n, Esq. Av. Carlos Hank González, Valle de Anáhuac, Ecatepec de Morelos C.P. 55210, Estado de México, Mexico; angel.hernandez@uaem.mx
3 Centro Nacional de Investigación y Desarrollo Tecnológico (CENIDET), Int. Internado Palmira S/N, Palmira, Cuernavaca C.P. 62490, Morelos, Mexico; guadalupe.ll@cenidet.tecnm.mx
* Correspondence: gurquiza@uaem.mx; Tel.: +52-01-777-3297084

Abstract: In this experimental work, a prototype of a hybrid solar–thermal–photovoltaic (HE-PV/T) heat exchanger has been designed, built, and characterized, with rectangular geometry and 12 fins inside, to obtain better heat flow and higher performance in order to achieve a better heat transfer coefficient, reducing and optimizing the working area. The heat exchanger contains 12 photovoltaic cells connected in series, with an angle of inclination of approximately 18° towards the south and a surface area of 0.22 m^2, smaller than those available on the market, which individually capture 147.05 W/m^2 as a photovoltaic panel and 240 W/m^2 as a solar collector. Mathematical models found in the literature from previous work were used for the electrical and thermal evaluations. The temperature of the PV cells was reduced to 13.2 °C and the thermal level of the water was raised to a temperature above 70 °C, with a photovoltaic–thermal coupling power of 307.11 W and a heat transfer coefficient of 5790 W/m^2 °C. The efficiencies obtained were as follows: thermal up to 0.78 and electrical up to 0.095. The novelty of these results was achieved in a reduced space of 40% less than those reported and available on the market.

Keywords: heat exchanger; thermal efficiency; photovoltaic cell; PH/T

Citation: Perez Grajales, S.G.; Hernández, A.H.; Juárez-Romero, D.; Lopez Lopez, G.; Urquiza-Beltran, G. Design, Construction, and Characterization of a Solar Photovoltaic Hybrid Heat Exchanger Prototype. *Processes* **2024**, *12*, 588. https://doi.org/10.3390/pr12030588

Academic Editors: Alvaro Antonio Ochoa Villa, Gustavo De Novaes Pires Leite and José Ângelo Peixoto Da Costa

Received: 24 October 2023
Revised: 6 March 2024
Accepted: 8 March 2024
Published: 14 March 2024

1. Introduction

1.1. Energy Situation

In today's industrial society, the scarcity of carbon-based fuels and their adverse effects on global warming and air pollution are issues of immediate concern [1,2]. The use mental awareness, and continuous improvements in renewable energy technology. In the long term, solar energy is currently the most affordable and abundant natural resource [3].

1.2. Solar Technology

Converting sunlight into direct current in solar cells or photovoltaic cells is one of the best ways to use solar energy to generate electricity [4,5]. The International Energy Agency (IEA) predicts that between 2022 and 2027, renewable energy capacity worldwide will increase by about 2400 gigawatts (GW), or almost 75% more than it is now [6]. The energy captured from the sun can be used where solar irradiation is attractive for the social necessities of a place, as it comes from a clean energy source and reaches thermal levels ranging from 60 to 280 °C and up to 400 °C using equipment already known for power generation systems [7]. The photovoltaic (PV) module currently has an overall efficiency of 5 to 20% [8]. It is the most common active method of obtaining electrical energy from direct solar irradiation. A porous coating was found to increase efficiency by 8.34% when thermal cooling of PV panels using porous media was studied numerically [9]. Majdi Hazami and others determined the technical performance in photovoltaic cells [10]. The cooling systems (water) manage to reduce the temperature of the photovoltaic panels, ranging from 6 to 20 °C and with improved electrical performance by up to 15.5% [11]. Hybrid solar collectors coated with low emissivity were manufactured for experimentation and simulation with silver. The thermal results obtained increased performance to −223.15 °C, while the electrical performance was reduced by only 3% [12]. Contrary to popular belief, increasing temperature impairs the efficiency of solar panels. The heat can reduce production efficiency by 10 to 25%, depending on where they are installed [13]. The relationship that exists between the amount of energy that arrives from space and that which is used by the panel is called instantaneous efficiency, which depends on the technology with which they are manufactured under international standards [14]. The combined solar systems were analyzed using the Taguchi method under five different climatic conditions to determine their optimal operating parameters. The results show that each parameter had a varying level of effect on performance at different locations [15]. The thermal performance of a parallel flow-based photovoltaic/thermal (PV/T) system was analyzed under the Malaysian composite climate. The new PV/thermal system was designed, developed, and studied, and the following results were obtained: The maximum thermal efficiency of the PV/T system was 76.58%, PV electrical efficiency was 9.89% and PV/T was 10.46% [16]. An experimental study has been carried out on a direct PV/T off-grid water heating technology. This is the first time that such a device has been tested experimentally, and its capacity to supply hot water at approximately 80 °C for a family of four has been demonstrated. The results obtained are as follows: electrical efficiency 13.4% and thermal 53.4% [17].

An experimental solar-assisted geothermal heat pump (SAGSHP) system for domestic heating applications using a series of vertical wells to seasonally store heat in an underground “geothermal energy bank” was studied and was able to meet the heating needs of the building in winter [18]. The most common liquid for cooling photovoltaic panels is water. Due to the characteristics of density (997 kg/m^3), specific heat capacity (4184 J/kg °C), and thermal conductivity (0.0006 W/m °C), to mention a few, it can also offer higher heat transfer coefficients for air [19]. There are different cooling techniques suitable for photovoltaic panels that depend on several factors, such as the type of photovoltaic panel, system layout, geometry, and climatic conditions [20]. The numerical performance of a solar-assisted heat pump coupled to a photovoltaic air heater was studied. The various geometric and operational parameters on the performance of an SAHP with AH-PV/T were carefully observed, and the feasibility of the project was demonstrated [21]. A novel photovoltaic thermal curtain wall (PV/T)-assisted dual-source heat pump (DSHP) system was proposed, which effectively integrates the PV/T system with the air-to-ground DSHP. The research was carried out through numerical simulation and experimental tests comparing it with a DSHP system without a curtain wall (PV/T) to explore the optimal mode of adaptation of solar energy [22]. They used the latent heat of evaporation to absorb the heat generated by the body of a PV module and reduce its temperature. Water was supplied to the back of the PV array from a gravity tank and a series of experiments in real conditions in the city of Riyadh demonstrated the effectiveness of the method. A reduction of more than 20 °C in the temperature of the PV panel and an increase of about 14% in the efficiency of electricity generation compared to a reference PV panel were achieved [23]. The performance of a low-priced prototype extruded heat sink for a low-concentration photovoltaic system was studied through various analytical correlations and CFD simulations and experimentally tested with temperature measurements at different points on the surface of the heatsink to select the most appropriate approach. Large deviations (up to 20 °C) of the base plate temperature were found from the correlations compared to the experimental results, probably due to the specific geometrical characteristics of the heat sink, with variable fin thickness and high fin length [24]. The researchers presented a model of a fin-cooled photovoltaic (PV) module under real operating conditions in which the potential of fins to control module temperature and improve electrical efficiency was evaluated and the attractiveness of such an arrangement compared to more established cooling techniques was confirmed [25]. Photovoltaic (PV) systems, which convert solar radiation directly into electricity, have made significant advances in scientific and commercial use. Efforts are being made to increase system efficiency and minimize costs [26]. Based on the literature, a passive cooling system composed of fins was designed and an overall evaluation of the fin-integrated photovoltaic modules was carried out to improve the overall performance. A collective experimental and simulation study was conducted to evaluate the effectiveness of the passive cooling system to mitigate the high module temperatures. The results of the 3 month experiment (October to March) showed an average overall efficiency increase of 5.47%, with a 40% reduction in the temperature coefficient for varying outdoor conditions [27]. With the development of distributed energy systems, photovoltaic panels are being incorporated into buildings to generate electricity from solar energy [28]. The efficiency of PV generation is typically around 15–20% but is still limited by the temperature of the module cells. For this purpose, cooling is applied as an effective method to improve efficiency [29]. There are reports that every 10 °C decrease in PV panel temperature could contribute to a 5% increase in PV cell efficiency [30]. To improve the efficiency of power generation, photovoltaic panels have been installed on the water surface to cool the photovoltaic cells [31]. Other photovoltaic panel cooling technologies include water spraying [32], evaporative cooling [33], pulsed heat pipes [34], and phase change material cooling [35], but they are not our objective in this work. A study on the impact of temperature on the performance of series- and parallel-connected monocrystalline silicon (mono-Si) solar panels was carried out using a solar simulator. Performance parameters such as open-circuit voltage, peak power, fill factor, and efficiency decreased with cell temperature, while short-circuit current increased [36]. After reviewing the literature, no work was found on these characteristics of the proposed configuration, which characterize a tubeless heat exchanger (HE) coupled to photovoltaic cells, saving space and increasing the energy level and other technical details (see initial specification). This experimental work investigated the coupling characteristics between heat exchangers and photovoltaic cells in solar systems to obtain their performance under ambient conditions, continuing a previous article [1]. This work aims to optimize the space of work equipment (hybrid panels), making them smaller and more efficient. The performance of the equipment can be obtained by analyzing solar thermal/photovoltaic hybrid systems. To this end, we designed and built a photovoltaic heat exchanger with rectangular flat-plate geometry (without tubes), with 12 pairs of fins along the plate to increase turbulence. This distinguishes it from other published works. In this case, monocrystalline photovoltaic cells have been connected at the top, which reduces the temperature through the fluid by taking advantage of the thermal levels and obtaining electricity, as mentioned above in the design of the heat exchanger. There is work from before this research, which is mentioned below: Some researchers have identified environmental and design parameters that influence the performance of such collectors, such as mass flow rate, inlet water temperature, absorber thermal conductivity, and absorber plate design parameters [37]. PV/T modules combine efficiencies from 40% to 87% and can be applied in ground, wall, and rooftop installations in urban and rural areas to supply energy [38]. The increase in temperature and decrease in efficiency has been analyzed using active and passive cooling methods. In these processes, water is normally used as the cooling medium [39]. A parameter investigation was carried out based on fin height, number, and distance between fins. The solar irradiance on the performance of the PV module was evaluated by CFD, ANSYS FLUENT, using 3D Navier–Stokes energy equations for numerical calculations [40]. An innovative hybrid photovoltaic evaporative cooling system (PV/EC) has been investigated in order to improve its efficiency by cooling the PV array, and this new design structure reduces the effect of solar radiation [41]. A photovoltaic–thermal (PV/T) array with a water-cooled heat sink was investigated and experimentally evaluated in the climatic conditions of the southern region of Iraq during summer. The water-cooled heat sink was applied to thermally manage the PV cells in order to increase the electrical output of the PV system. The effects of solar irradiation on average PV temperature, electrical power, and overall electro thermal efficiency were investigated [42]. An investigation was conducted on the heat transfer coefficient (HTC) of a tube heat exchanger (HPHE) while installed as a cooling mechanism in photovoltaic panels. The experiment monitored the effect of temperature variations on the power generation induced by the PV-HPHE [43]. In this section, we have commented on the works published in the literature on the energy situation and the advances in solar technology today, as well as the different forms or configurations of experimental work carried out in large spaces with respect to our equipment, in which we have optimized to 40% less compared to those [37,44], reported in the literature and those existing on the market, which have a totally different geometry than those studied, achieving equivalent results (with a small team). In addition to focusing on different heat exchanger designs, the experimental research results were based on the performance of the hybrid thermal–photovoltaic system as well as its temperature.

2. Method

2.1. Location of the Study

Table 1 shows the geographical coordinates of the experimental laboratory and the national water system where the meteorological data needed for our project were provided.

Table 1. Location of the institutions involved in the project implemented.

	Autonomous University of the Morelos State (CIICAP-UAEM)	**National Water Commission (CONAGUA)**
Altitude (masl)	1897	1610
Longitude (°)	−99.23	−99.21
Latitude (°)	18.88	19.01

2.2. Design of the Heat Exchanger

The photovoltaic cells were purchased from DAH Solar (Anhui Daheng Energy Technology) Co., Ltd., in Hefei, China. The aluminum used in the heat exchanger was acquired from ABC Aluminum Solutions located in La Cuestesita, San Antonio de los Buenos, 22563 Tijuana, B.C., Mexico. For the elaboration of the prototype, 12 monocrystalline cells were used with an efficiency of 16.64%, given by the laboratory of origin. These were attached to a finned heat exchanger made of aluminum. The fins and aluminum enhance the heat transfer coefficient. Figure 1a shows the top of the heat exchanger where the photovoltaic cells are fixed. Figure 1b shows the internal part of the heat exchanger where the water passes through, which extracts the heat received by the cells provided by solar radiation. It was designed, built, and characterized with aluminum with a flat rectangular geometry with 12 pairs of fins inside one of the two plates [45] to improve the turbulence through which the water circulates, acting as a temperature absorber in the photovoltaic cells. This type of experimental prototype allows a heat transfer that favors thermal exchange between the environment and the coupling device, thus reducing the temperature of the solar cell and improving its performance.

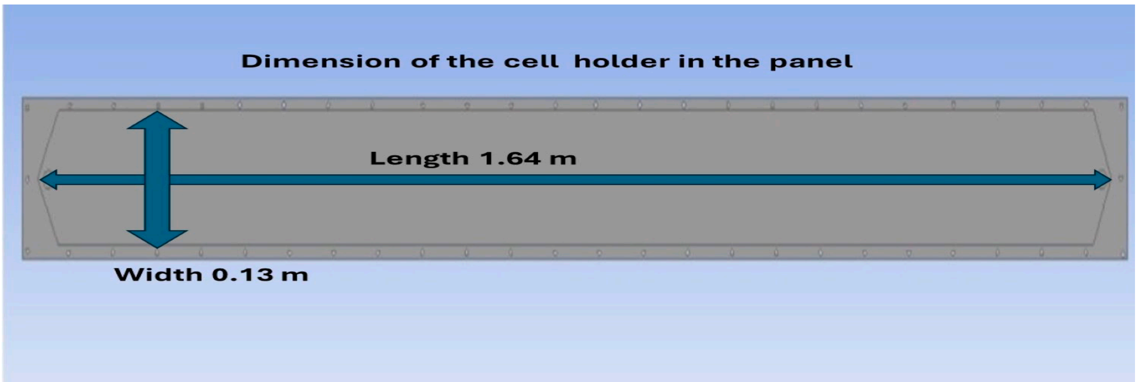

(**a**)

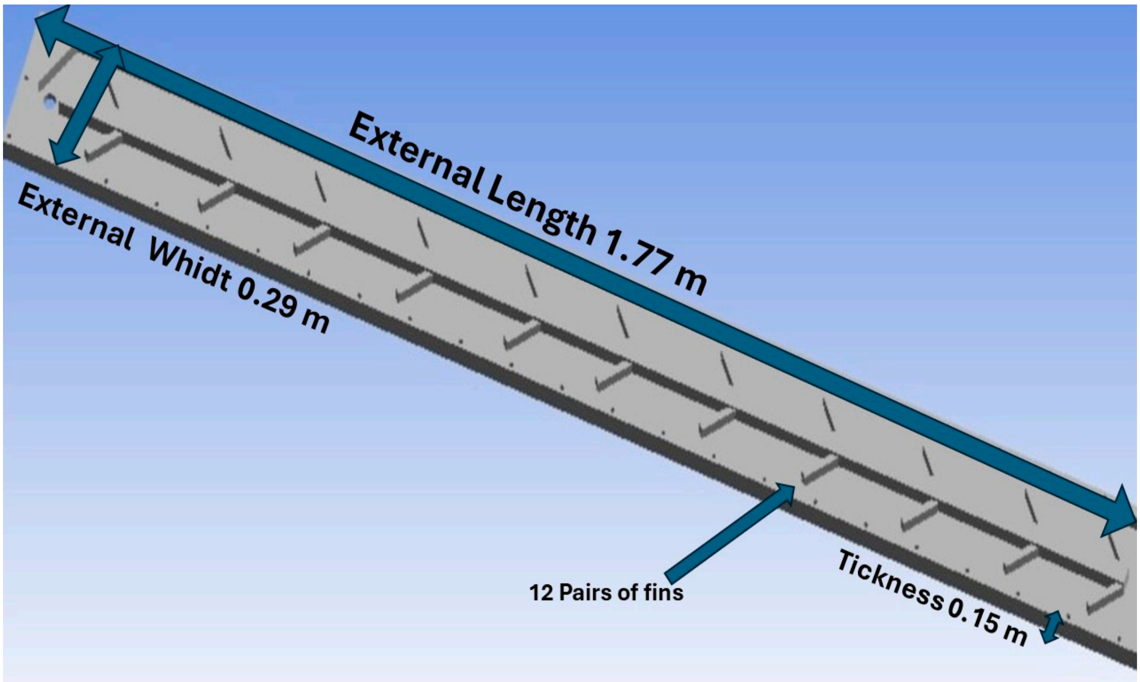

(**b**)

Figure 1. (**a**) Upper-view of the heat exchanger. (**b**) Internal view and external dimensions of the heat exchanger.

2.3. Installation and Instrumentation of the Heat Exchanger and Photovoltaic Cells

Figure 2a,b show the design of the experimental working device. It has an angle of inclination towards the south of approximately 18° (SP) and is connected to a cylindrical tank at both ends by copper pipes that allow the fluid to reach the inlet and outlet of the solar panel. See Table 2 for more details:

Table 2. Interconnection of equipment.

	Length (m)	Diameter (m)	Capacity (L)	Power (kW)
Tank	0.79	0.39	100	-
Pump	-	-	-	0.74
Copper pipes	-	0.02	-	-

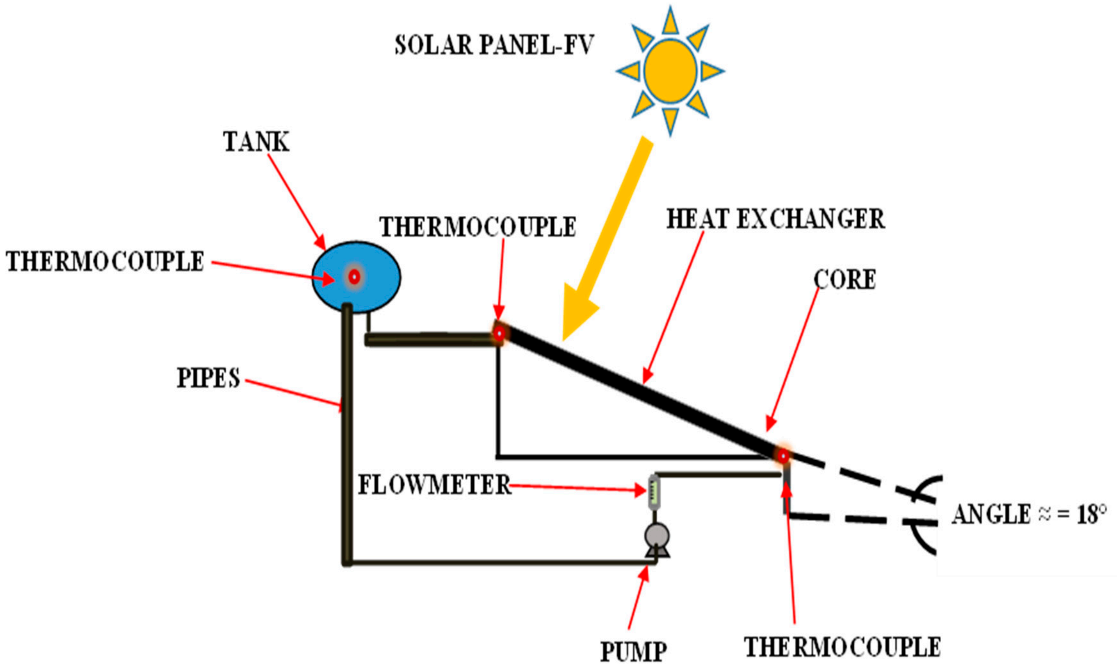

(**a**)

(**b**)

Figure 2. (**a**) Design of the coupled equipment. (**b**) Experimentally coupled equipment.

2.4. Experimental Methodology

Methodology: Water is circulated using a pump from the solar panel to the storage tank. After the water has been circulated repeatedly, it returns to the storage tank with increased temperature due to thermal absorption from the solar panel. The cycle is repeated, resulting in the desired thermoelectric cogeneration for use in domestic and other services. Instrumentation: Cole Parmer flow meter model 32044-00, with a 5 to 65 mm scale, a 1 mm resolution, and an accuracy of ±2% of the full scale for thermal fluid. Measurements were supplied with a polycarbonate cover, a precision adjustment valve and

316 stainless steel floats, with a maximum pressure of 200 psi, a temperature range from −26 to 121 °C, and a volumetric flow from 7 to 150 mL/min. Temperature measurements were performed using 4 T-type thermocouples (copper-constantan), which can measure temperatures between −200 and 400 °C with an accuracy of ±0.5 °C, are useful in reducing and oxidizing environments, and are also resistant to corrosion in humid atmospheres. These thermocouples were installed in thermowells, with Parker-brand model FBZ 44 connectors made of 316 stainless steel material and welded tube with a 6.3 mm (1/4 inch) outside diameter and 30.0 mm in length. Electrical measurements were taken 2 h after the start of the tests (12:15 h), when the action of solar radiation reached its peak on the hybrid exchanger. The following values were recorded: open-circuit voltage, short-circuit current, and temperature of the photovoltaic cells. The current-voltage curve measurements were performed with the Solmetric 3 PV Analyzer 7 - 2018 software, which allows the I-V curves of the solar panels to be measured (which is essential for evaluating their performance and detecting possible problems) and the analyzer to be directly connected to the PV modules to obtain accurate data. The PV Analyzer software provides tools to analyze the collected data. You can examine the I-V curves, identify the maximum power points, and check the quality of the system. PV Analyzer works best with Microsoft Windows 10 or Windows 11 with all recommended updates. Calibration of the flowmeter was performed by means of a test bench. This consisted of placing the stem on the operating scale, circulating water through it, capturing it for one minute, and repeating this operation up to three times; then weighing it and deducting the weight of the collecting tanks; and finally obtaining a correlation. A Cole–Parmer thermostatic bath with a temperature range of −45 °C to 200 °C, a stability of ±0.1, °C and an accuracy of ±0.25 °C was used to calibrate the thermocouples. Each temperature range was compared with the calibration standard at the above temperatures when there were no temperature variations and for a period of 5 min. The correlation equation was calculated with the averages of each calibration point and the standard temperature for each thermocouple. The following were used for the system acquisition data: BK PRECISION power supply, model 1670A DC 127 60 Hz, multiplexer card, Agilent Technology model 34901A, model 34970, and HP Bench Link data logger software. The thermal model is based on the useful energy of the collector, and the energy captured by the heat transfer fluid is the difference between the total incident energy and the lost energy, the total incident energy being the sum of the energies produced by direct, diffuse, and reflected radiation, where Q is the useful energy, Q_1 is the total incident energy, and Q_2 is the lost energy. The incident energy Q_1 is the product of the radiant energy intensity (G) times the surface area (A). But not all the incident energy is absorbed. Due to the transmittance of the cover (τ) and the absorption coefficient (α) of the absorber plate, the fraction of energy actually absorbed is in terms of lost energy Q_2, The detailed calculation is very complex since it depends on different proportions on the losses by radiation, convection, and conduction. The average temperature of the absorber plate cannot be calculated in a simple way, but the average temperature T_m of the heat transfer fluid when it flows through the collector under the absorber plate can be determined with sufficient accuracy by finding the average of the temperature of the heat transfer fluid at the inlet and outlet of the collector. If the absorber plate temperature is replaced by the fluid temperature, it is necessary to introduce a correction factor, FR, called the efficiency factor or heat transport coefficient. In this way, the useful energy equation is transformed into what is known as the Bliss equation: The collector efficiency is defined as the ratio between the energy captured and the energy received at a given instant. For the photovoltaic thermal model, it is based on three parts: energy balance of the solar cells, energy balance in the absorber plate, and energy balance of the fluid. For this, the balance in the solar cells is based on the heat flow that reaches the cells, subtracting the heat flows by radiation from the cells to the environment and by convection and conduction to the environment minus the flow converted into electricity. In the case of the absorber plate, the balance is obtained by subtracting the conduction heat fluxes from the cell to the plate, from the plate to the environment, and finally from the plate to the fluid. The energy balance of

the fluid is based on the conduction heat flow from the fluid to the environment plus the heat flow. Figure 3 details the experimental methodology through the flow diagram, which consisted of subtracting the temperature gained from the photovoltaic cells as a product of solar radiation with respect to the ambient temperature, and then proceeding to subtract the temperature of the water that was absorbed from the cells to the difference of the two previous temperatures, obtaining the following results: thermal heat gained by the fluid from the photovoltaic cells and thermal and electrical efficiency. Finally, the developed photovoltaic thermal model was successfully verified by the experimental results.

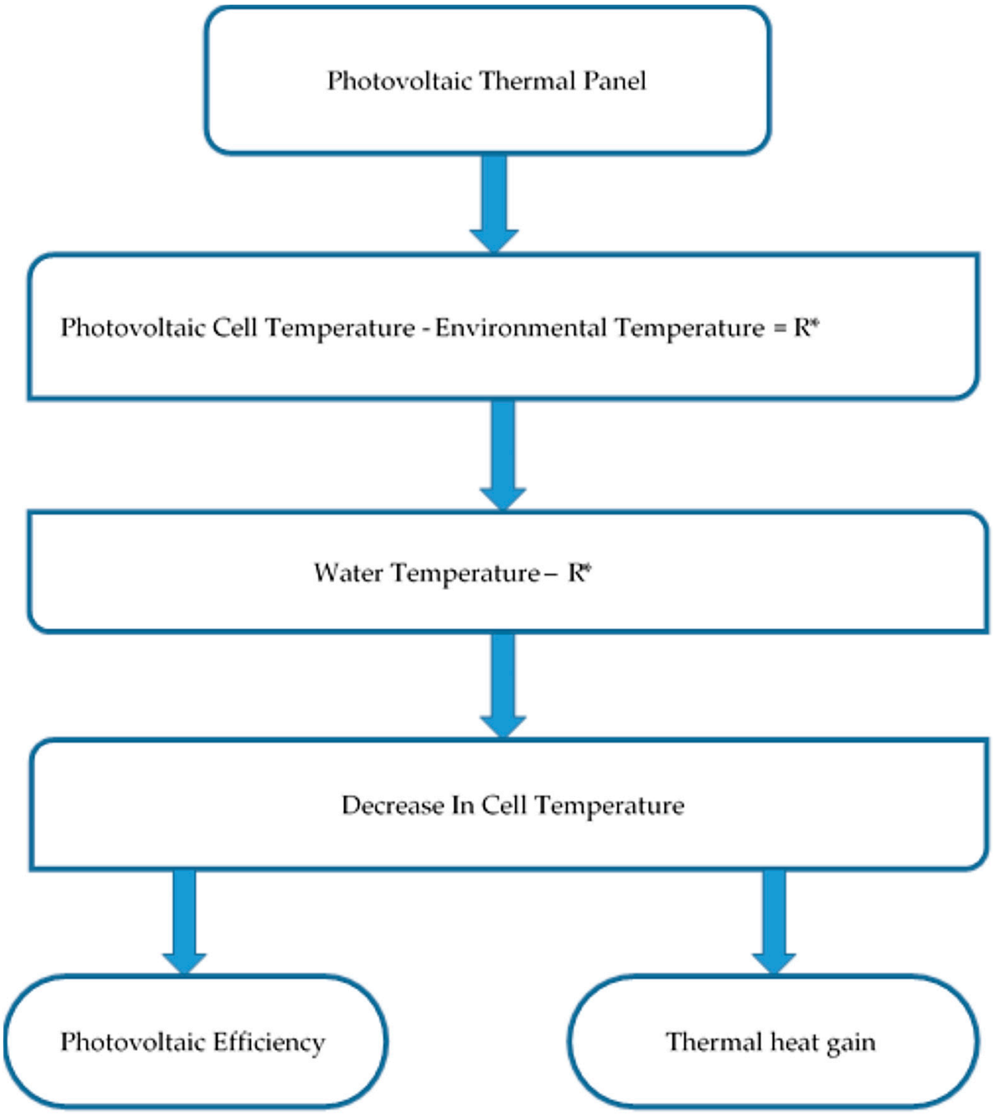

Figure 3. Flow chart of the experimental methodology.

2.5. Calculation of the Heat Exchanger (HE) or Solar Thermal Collector

The thermal efficiency of the HE is defined as the relationship between the energy captured and the energy received at a given time.

$$\eta = Q_u / G \cdot A \tag{1}$$

Substituting Q_u for its value, in the Bliss equation [46], we have:

$$\eta = \frac{\dot{m} \cdot C_p (T_{out} - T_{in})}{G \cdot A} \tag{2}$$

where:

$$Q_u = \dot{m} \cdot C_p (T_{out} - T_{in}) \tag{3}$$

2.6. Calculation of the Components of the Photovoltaic Cells

The equations for these individual components were developed from energy balance, photoelectric conversion, thermal conductivity, convection, and radiation analyses [47]. To calculate the effect of temperature on the photovoltaic cells (T_t):

$$T_t = T_a + K \cdot R \tag{4}$$

To calculate the operating power (P_o):

The temperature increase is determined with a test reference at (25 °C).

Where:

$$P_t = P_p - \left(P_p \cdot \delta \cdot \Delta T\right) \tag{5}$$

Efficiency of the photovoltaic conversion solar cell in the equation [48]:

$$\eta_{Pv} = \frac{I_{max} \cdot V_{max}}{G \ \cdot \ A} \tag{6}$$

2.7. Photovoltaic Thermal Model

Figure 4 shows this photovoltaic thermal model describing heat transfer (conduction, convection, and radiation). When solar radiation comes into contact with the heat exchanger cells, part of it bounces back to the environment and the other part is absorbed by the cells, causing them to increase their temperature so that the heat transfer fluid is responsible for absorbing it, converting it into thermal energy. But at the same time, there is a release of energy to the environment through conduction and convection that occurs inside the coupled solar equipment to produce the desired products (heat and electricity). The process takes place in three parts, represented by a photovoltaic panel (plate), solar cells, and fluid (water).

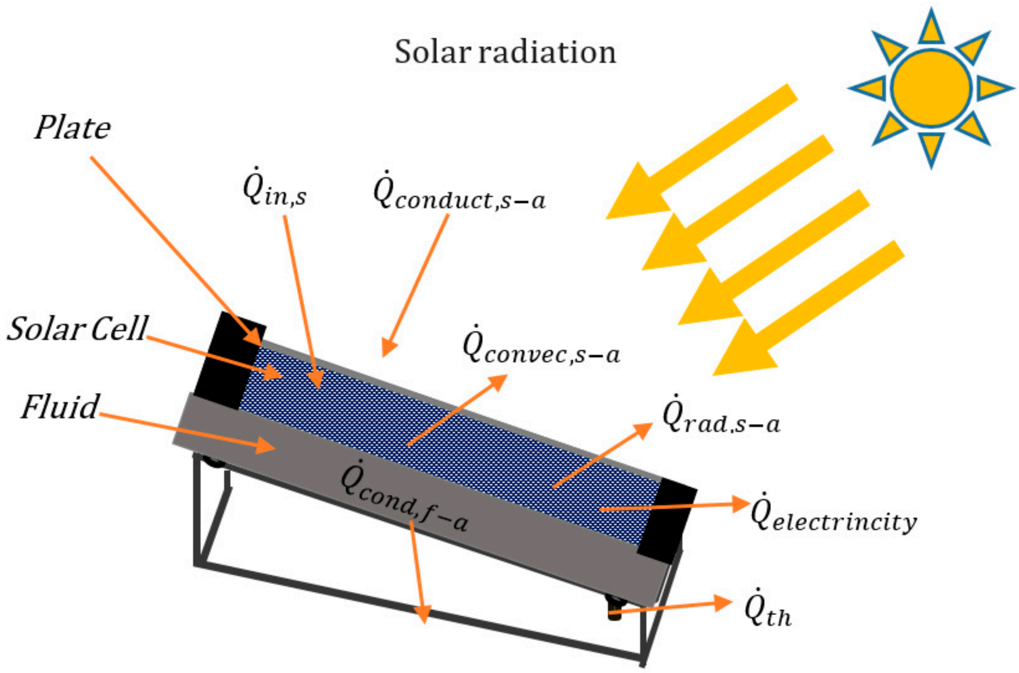

Figure 4. Photovoltaic thermal model.

2.8. Thermal Energy Balance for Solar Energy Generation

The equations for each of these components are based on energy balance analysis, photoelectric conversion, thermal conductivity, convection, and radiation, and include panel absorbance (α_s); solar radiation (G); panel surface area (A_s); ambient temperature (T_a); heat transfer coefficients rad, convec, and conduct (fi_{rad}, h_{convec}, $\text{fi}_{conduct}$); solar cell (S); and plate temperature (T_p) [44].

Energy balance for solar cells:

$$\dot{Q}_{be,S} = \dot{Q}_{in,s} - \dot{Q}_{rad,s-a} - \dot{Q}_{convec,s-a} - \dot{Q}_{conduct,s-a} - \dot{Q}_{electricity}$$
$$\dot{Q}_{be.S} = \alpha_s \cdot A_s \cdot G - A_s \cdot \text{fi}_{rad} \cdot (T_s - T_a) - A_s \cdot h_{convec}(T_s - T_a) - A_s \cdot \text{fi}_{conduct} \cdot (T_s - T_p) - \eta_s \cdot \alpha_s \cdot G \cdot A_s \quad (7)$$

Energy balance for the absorber plate:

$$\dot{Q}_{be,P} = \dot{Q}_{conduct,\ s-p} - \dot{Q}_{conduct,p-a} - \dot{Q}_{conduct,P-f}$$
$$\dot{Q}_{be,P} = A_s \cdot \text{fi}_{conduct} \cdot (T_s - T_p) - A_s \cdot \text{fi}_{conduct} \cdot (T_p - T_a) - q_f \quad (8)$$

Energy balance for the fluid:

$$\dot{Q}_{be,f} = \dot{Q}_{conduct,f-a} + \dot{Q}_{th}$$
$$\dot{Q}_{be,f} = A_f \cdot \text{fi}_{conduct} \cdot \left(T_f - T_a\right) - \dot{m} \cdot C_P \cdot \left(T_{fo} - T_{fi}\right) \quad (9)$$

The total performance of the entire system is the result of the individual division and addition of each of them [45,47].

$$\eta_{Pv/Th=}\ \eta_{Pv} + \eta_{Th} \quad (10)$$

where:

$$\eta_{Pv/Th} = \frac{I_{max} \cdot V_{max}}{G \cdot A} + \frac{\dot{m} \cdot C_p (T_{out} - T_{in})}{G \cdot A} \quad (11)$$

3. Results and Discussion

The tests were carried out during May 2019, the month of highest radiation in Mexico. The tests began by capturing the greatest amount of solar energy at 10:00 a.m. and concluded at 4:00 p.m. Figure 5 shows the experimental results (1089 data points) for HE-PV/T, highlighting the influence of the maximum solar radiation of 1067 W/m^2 (this radiation can be observed in detail in Figure 6), with a constant of mass flow of 0.01 kg/s. The temperature of the solar cell reached 73.61 °C as a result of the solar radiation absorbed by the cell, and the extractor fluid that passed under the cell for cooling reduced this temperature by approximately 13.18 °C as the final product. This resulted in a cell temperature of 60.4 °C, and consequently, the water absorbed all the heat from the cells, resulting in a thermal temperature of 73.6 °C. In addition, this increases the useful life of the hybrid system because it is not subjected to high temperatures. The thermal coupling power at the end of the experiment was 307.11 W. These results are due to the fact that the heat exchanger was designed and built with a flat, rectangular internal geometry containing 12 pairs of fins along the plate with the purpose of increasing thermal performance. The experimental prototype allows for heat exchange between the environment and the attached equipment, reducing the temperature of the photovoltaic cells to increase their performance.

Figure 6 shows the power of the solar cell as a function of solar radiation. The power reached approximately 27 W between 12 and 13 h and then decreased when exposed to solar radiation to 18 W. This means that when solar radiation increases, it is advisable to have a cooling system to improve performance. Also, the quality of the cells in which they were manufactured has to be considered.

Figure 7 shows the average of a series of experimental tests in which the efficiency of the photovoltaic cells was calculated during the spring in May, evaluating the effect of solar irradiation on the cells. The result was 0.095, compared to 0.166 in the manufacturer's laboratory. This indicates that the tests performed in the manufacturer's laboratory will not give the same results as in the experimental field because the conditions under which the panels operate are different. Table 3 shows the comparison of the manufacturer's results with the experimental results.

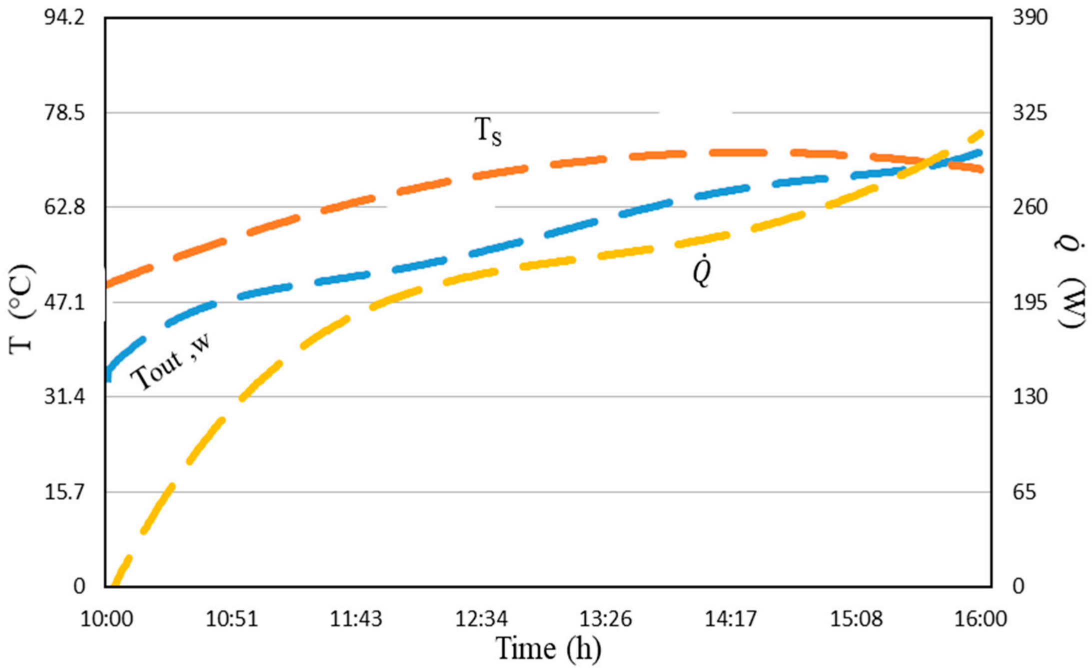

Figure 5. Behavior of the temperature of the solar system coupling (May 2019).

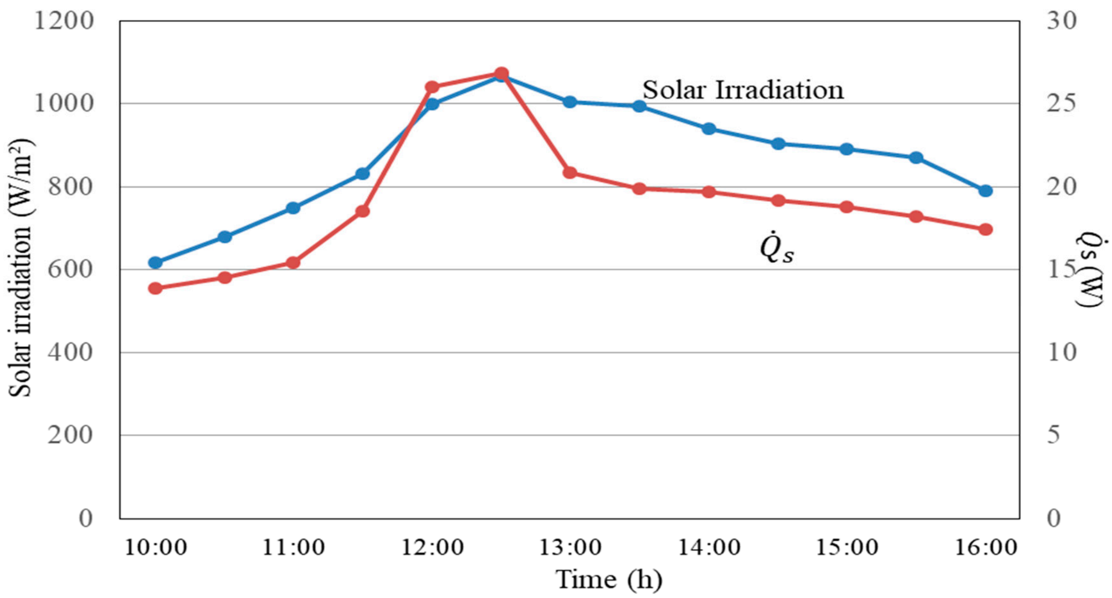

Figure 6. Solar cell power vs. solar irradiance.

Figure 8 of this graph shows that the ambient temperature depends on the day and month of the year concerning the radiation received, so it can be said that the greater the temperature differences between the solar panel and the ambient temperature, the lower the overall efficiency of the panel. The yield obtained was 0.095, and this was due to the dimensions of the storage tank, which was small, with a capacity of 100 L, which did not allow for further improvement in the performance of the solar cell because at approximately 4:00 p.m. the temperature stabilized throughout the solar system.

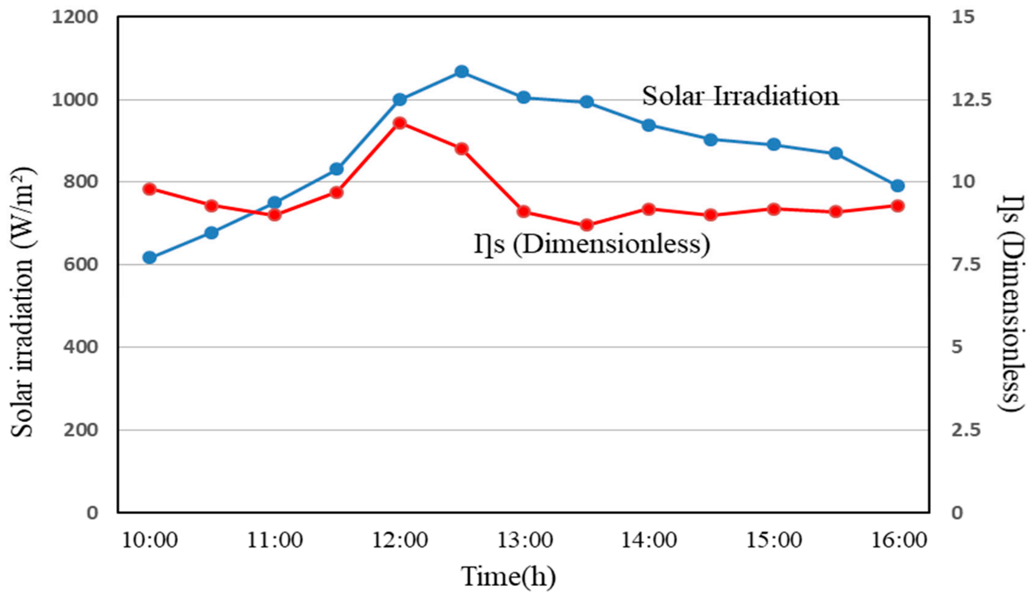

Figure 7. Cell efficiency vs. solar irradiance.

Table 3. Comparison of the manufacturer's results with the experimental results.

Comparison of Results		
Monocrystalline Cells		
	Manufactured in China	**Experimental**
Efficiency	0.16	0.095
Irradiation	1000 W/m^2	1067 W/m^2
Environment temperature	25.00 °C	31.90 °C
Maximum power current	5.40 A	4.21 A
Maximum power voltage	6.00 V	5.82 V

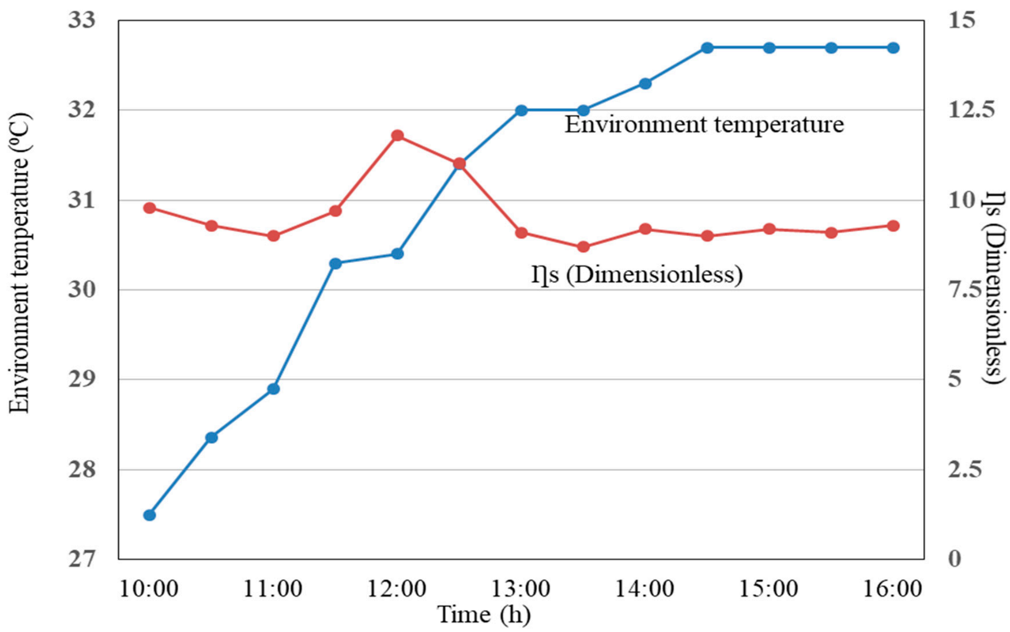

Figure 8. Cell efficiency vs. environmental temperature.

The experimental tests were carried out in spring, with the highest solar radiation of the month captured in the laboratory area. The main parameter was the thermal efficiency of the solar panel, represented by a curve in Figure 9, which is a function of temperature and the solar radiation received. The maximum result obtained was 0.78 at an ambient temperature of 32.7 °C. In the SP configuration, NOM003-ENER-2011 [49] and ANSI/ASHRAE 93-1986 [50] procedures were carried out to determine the efficiency.

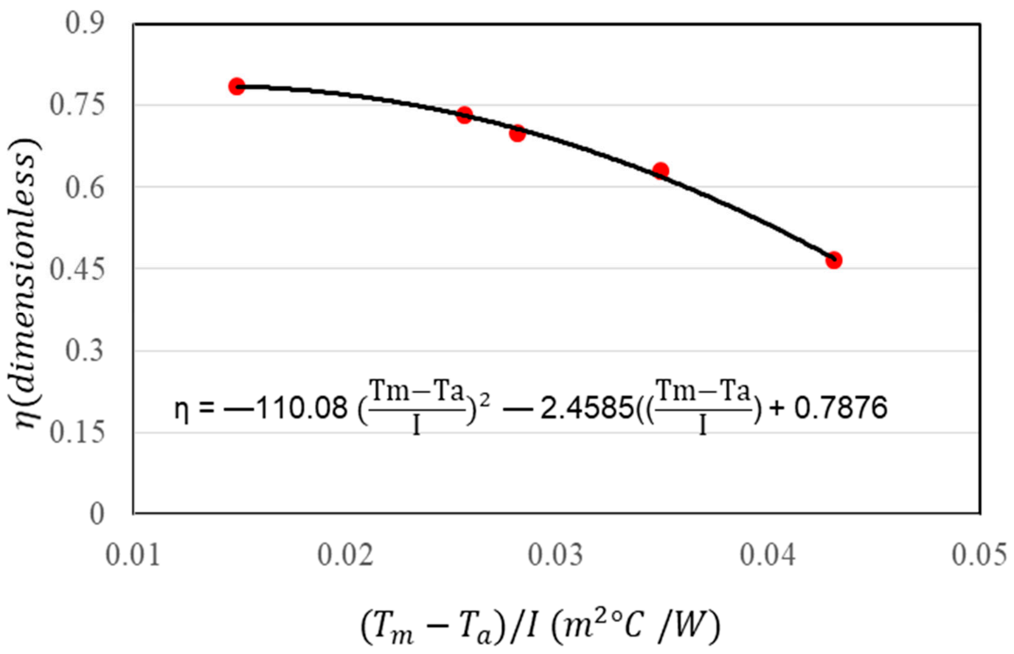

Figure 9. The efficiency of the HE-FV/T.

Table 4 shows the operating parameters of the coupled system at the end of the experiment that were obtained (outlet water temperature, power of the 12 photovoltaic cells) at approximately 4:00 p.m.

Table 4. HE-PV/T performance results for May 2019.

Data	
$T_{out,\ w\ (4{:}00\ PM)}$	73.61 °C
$T_{finish,\ s\ (4{:}00\ PM)}$	60.43 °C
$\dot{Q}_{th\ (4{:}00\ PM)}$	307.11 W
η_s η_{th}	0.095 0.78
$\dot{m}_{steady}$	0.01 kg/s

3.1. Calculation of Uncertainty for Coupling

The combined measurement uncertainty reinforces the process of obtaining confidence in the results to validate the work by allowing the comparison of different measurements. This combined measurement was obtained using the Taylor series method [51]. This determines the uncertainty of the combination of large-scale direct and indirect variables provided by the manufacturer, where "y" is given by a model y = f(X_1, X_2, X_N) and the combined uncertainty Uc (y) is given by $U^2{}_C$ (y) = $\Sigma^N{}_{i=1}$ $(\partial f/\partial x_i)^2$ U^2 (X_i), which was used to determine the coupling uncertainty and, therefore, the uncertainty of the external thermal load of the solar heat exchanger: temperature of the hot water ± 0.04%, mass flow rate of hot water ± 0.03%, and thermal heat flow ± 7.4%.

3.2. Final Remarks

We observed that our results were satisfactory, obtaining electricity and hot water in a device with reduced geometrical characteristics that has 12 pairs of fins inside with a mass flow mentioned in the Results and Discussion sections, compared to those reported, which were larger in size. But we also need to improve the performance of the photovoltaic cells, as we believe that the transport from the place of origin where we acquired them may have interfered in obtaining better performance of the cells (they may have been damaged). To conclude our observations, our prototype has the characteristics of our research, as there is no other in the literature with the same geometrical dimensions. The storage tank requires a larger volume for better thermal evaluation. This equipment could be marketed in the future in residences or private homes, since the products obtained from this equipment are equivalent to those currently available on the market, which are much larger in size.

4. Conclusions

In this experimental work, a prototype of a hybrid solar–thermal–photovoltaic (HE-PV/T) heat exchanger was designed, built, and characterized with the measurements described above, which is unique since there is no other similar one reported in the literature. With the same measurements an the same characteristics, the results were as follows: The cell temperature decreased by approximately 13.2 °C due to the absorption of heat by the cooling fluid, thus increasing the fluid temperature by more than 70 °C by the end of the test. The thermal efficiency of the coupling reached 0.78, with a maximum water temperature of 73.6 °C. The operating temperature of the solar cell was 68 °C and its output power was 26.83 W. The overall heat transfer coefficient was 5790 W/m^2 °C. In the coupling, 307.11 W of heat flow were obtained, with an electrical efficiency of 0.095. This value is considered acceptable since in the literature there are reports that start at 0.09 in monocrystalline cells such as those used in this work, yielding a total efficiency of 0.88 for the fully coupled system. It was proven that when cooled by forced convection the cells have better performance, since the flow is constant thanks to the pump. This designed, built, and evaluated prototype managed to make a difference with respect to those previously published in scientific journals since this small team achieved the following contributions to science: The area of the heat exchanger was reduced by 40% compared to those existing on the market, which was one of the main objectives, and equivalent results were obtained. The fins that were added to the interior were used to improve the heat transfer in combination with mass flow and thus have excellent thermal performance.

Author Contributions: S.G.P.G.: Writing—original draft, investigation, methodology, A.H.H.: investigation, writing. D.J.-R.: English reviewer, methodology. G.L.L.: methodology. G.U.-B.: investigation, supervision, and review & editing. All authors have read and agreed to the published version of the manuscript.

Funding: This research received no external funding.

Data Availability Statement: The data is not available due to the privacy of the authors but, if anyone is interested, they can send me their request to the e-mail sandro.perez@uaem.mx.

Acknowledgments: I thank the National Council of Humanities, Sciences, and Technologies (CONAHCYT) for supporting me with the Postdoctoral Fellowship and fulfilling my goals as a researcher in training.

Conflicts of Interest: The authors declare that there is no conflict of interest.

Abbreviations

Symbol or Abbreviation	**Description**
A	Total useful irradiance of the panel surface [kW/m^2]
A_S	PV panel area [m^2]
Cp	Heat capacity [J/(kg °C)]
Connect	Convection
Conduct	Conduction
Electricity	Electricity output
h	Heat transfer coefficient [W/m^2 °C]
I	Current [A]
K	Coefficient of variation [^{0}C. cm^2/mW]
$\dot{m}$	Mass flow [kg/s]
P	Output power at a working temperature [W]
P*pP*	Panel peak power (25 °C)Plate
PV/T	Photovoltaic thermal system
Q	Energy [W]
$\dot{Q}$	Heat flow rate of power [kW]
Qu	Amount of useful energy extracted per area [kW/m^2]
rad	Radiance
R	Solar radiation in mW/cm^2 [varies between 80 and 100 mW/cm^2]
R*	Difference of solar cell temperature minus ambient temperature
S	Solar cell
GT	Incident solar radiation absorbed by area [W/m^2]Temperature [°C]
V	Voltage [V]
Subscripts	
a	Environment
be	Energy balance
electricity	Electricity
Pv, *in*	Photovoltaic panel input
f	Fluid
in	Inlet
max	Maximum
out	Outlet
P_{IN}	Input power
SP	Solar panels
s-a	Output of the photovoltaic panel to the environment
s	Solar cell
t	Work
wall	Wall
w	Water
Greek Letters	
$\alpha\alpha_s$	Vessel or panel absorbance (dimensionless)PV panel absorptivity
$\Delta\Delta$t	DeltaTemperature increase above 25 °C (Tt − 25 °C)
Δ	Degradation coefficient
η	Efficiency (dimensionless)
Λ	Thermal conductivity [W/(m°C)]
T	Transmittance of glass cover [dimensionless]

References

1. Perez, S.G.; Huicochea, A.; Urquiza, G.; Hernandez, A.H.; Siqueiros, J. The commissioning of absorption heat transformer for water distillation using solar panels. *Desalination Water Treat.* **2020**, *204*, 22–32. [CrossRef]
2. Hernández, T.; Pérez, S.G.; Flores, O.; Hernández, J.A.; Juárez-Romero, D.; Álvarez, A.; Galaviz-Rodriguezc, J.V. Heat transfer prediction on flat solar collectors for the water purification system integrated into an absorption heat transformer. In Proceedings of the EDS Conference on Desalination for the Environment: Clean Water and Energy, Rome, Italy, 22–26 May 2016; Volume 22, p. 26.
3. Awasthi, A.; Shukla, A.K.; SR, M.M.; Dondariya, C.; Shukla, K.N.; Porwal, D.; Richhariya, G. Review on sun tracking technology in solar PV system. *Energy Rep.* **2020**, *6*, 392–405. [CrossRef]
4. Al-Ezzi, A. The market of solar panels in the United Kingdom. *Appl. Sol. Energy* **2017**, *53*, 78–84. [CrossRef]

5. Nayak, P.K.; Mahesh, S.; Snaith, H.J.; Cohen, D. Photovoltaic solar cell technologies: Analyzing the state of the art. *Nat. Rev. Mater.* **2019**, *4*, 269–285. [CrossRef]
6. Enlight. Energía Solar: Perspectiva 2023 en México, y el Mundo. 2023. Available online: https://www.enlight.mx/blog/energia-solar-perspectiva-2023-en-mexico-y-el-mundo (accessed on 13 October 2023).
7. del Amo, A.; Martínez-Gracia, A.; Bayod-Rújula, A.A.; Antoñanzas, J. An innovative urban energy system constituted by a photovoltaic/thermal hybrid solar installation: Design, simulation and monitoring. *Appl. Energy* **2017**, *186*, 140–151. [CrossRef]
8. Grubišić-Čabo, F.; Nižetić, S.; Giuseppe Marco, T. Photovoltaic panels: A review of the cooling techniques. *Trans. FAMENA* **2016**, *40*, 63–74.
9. Essa, M.A.; Talaat, M.; Amer, A.; Farahat, M.A. Enhancing the photovoltaic system efficiency using porous metallic media integrated with phase change material. *Energy* **2021**, *225*, 120299. [CrossRef]
10. Hazami, M.; Riahi, A.; Mehdaoui, F.; Nouicer, O.; Farhat, A. Energetic and energetic performance analysis of a PV/T (photovoltaic thermal) solar system tested and simulated under Tunisian (North Africa) climatic conditions. *Energy* **2016**, *107*, 78–94. [CrossRef]
11. Hasanuzzaman, M.; Malek, A.B.M.A.; Islam, M.M.; Pandey, A.K.; Rahim, N.A. Global advancement of cooling technologies for PV systems: A review. *Sol. Energy* **2016**, *137*, 25–45. [CrossRef]
12. Lämmle, M.; Kroyer, T.; Fortuin, S.; Wiese, M.; Hermann, M. Development and modeling of highly efficient PVT collectors with low-emissivity coatings. *Sol. Energy* **2016**, *130*, 161–173. [CrossRef]
13. Greentech Renewables. Available online: https://www.greentechrenewables.com/article/how-does-heat-affect-solar-panel-efficiencies (accessed on 13 October 2023).
14. Elibol, E.; Özmen, Ö.T.; Tutkun, N.; Köysal, O. Outdoor performance analysis of different PV panel types. *Renew. Sustain. Energy Rev.* **2017**, *67*, 651–661. [CrossRef]
15. Li, Y.H.; Kao, W.C. Taguchi optimization of solar thermal and heat pump combi systems under five distinct climatic conditions. *Appl. Therm. Eng.* **2018**, *133*, 283–297. [CrossRef]
16. Hossain, M.S.; Pandey, A.K.; Selvaraj, J.; Abd Rahim, N.; Rivai, A.; Tyagi, V.V. Thermal performance analysis of parallel serpentine flow-based photovoltaic/thermal (PV/T) system under composite climate of Malaysia. *Appl. Therm. Eng.* **2019**, *153*, 861–871. [CrossRef]
17. Cen, J.; du Feu, R.; Diveky, M.E.; McGill, C.; Andraos, O.; Janssen, W. Experimental study on a direct water heating PV-T technology. *Sol. Energy* **2018**, *176*, 604–614. [CrossRef]
18. Naranjo-Mendoza, C.; Oyinlola, M.A.; Wright, A.J.; Greenough, R.M. Experimental study of a domestic solar-assisted ground source heat pump with seasonal underground thermal energy storage through shallow boreholes. *Appl. Therm. Eng.* **2019**, *162*, 114218. [CrossRef]
19. Mah, C.Y.; Lim, B.H.; Wong, C.W.; Tan, M.H.; Chong, K.K.; Lai, A.C. Investigating the performance improvement of a photovoltaic system in a tropical climate using the water-cooling method. *Energy Procedia* **2019**, *159*, 78–83. [CrossRef]
20. Elavarasan, R.M.; Mudgal, V.; Selvamanohar, L.; Wang, K.; Huang, G.; Shafiullah, G.M.; Nadarajah, M. Pathways toward high-efficiency solar photovoltaic thermal management for electrical, thermal and combined generation applications: A critical review. *Energy Convers. Manag.* **2022**, *255*, 115278. [CrossRef]
21. Choi, H.U.; Choi, K.H. Numerical study on the performance of a solar-assisted heat pump coupled with a photovoltaic-thermal air heater. *Energy* **2023**, *285*, 129480. [CrossRef]
22. Chang, S.; Feng, G.; Zhang, L.; Huang, K.; Li, A. Multi-objective optimization of a photovoltaic thermal curtain wall-assisted dual-source heat pump system. *Appl. Therm. Eng.* **2023**, *222*, 119845. [CrossRef]
23. Haidar, Z.A.; Orfi, J.; Kaneesamkandi, Z. Experimental investigation of evaporative cooling for enhancing photovoltaic panels efficiency. *Results Phys.* **2018**, *11*, 690–697. [CrossRef]
24. Gallero, F.J.G.; Maestre, I.R.; Hemida, H.; Gómez, P.Á. Practical approaches to assess thermal performance of a finned heat sink prototype for low concentration photovoltaics (LCPV) systems: Analytical correlations vs CFD modelling. *Appl. Therm. Eng.* **2019**, *156*, 220–229. [CrossRef]
25. Vittorini, D.; Cipollone, R. Fin-cooled photovoltaic module modeling–Performances mapping and electric efficiency assessment under real operating conditions. *Energy* **2019**, *167*, 159–167. [CrossRef]
26. Al Hariri, A.; Selimli, S.; Dumrul, H. Effectiveness of heat sink fin position on photovoltaic thermal collector cooling supported by paraffin and steel foam: An experimental study. *Appl. Therm. Eng.* **2022**, *213*, 118784. [CrossRef]
27. Raina, G.; Sinha, S.; Saini, G.; Sharma, S.; Malik, P.; Thakur, N.S. Assessment of photovoltaic power generation using fin augmented passive cooling technique for different climates. *Sustain. Energy Technol. Assess.* **2022**, *52*, 102095. [CrossRef]
28. O'Shaughnessy, E.; Cutler, D.; Ardani, K.; Margolis, R. Solar plus: A review of the end-user economics of solar PV integration with storage and load control in residential buildings. *Appl. Energy* **2018**, *228*, 2165–2175. [CrossRef]
29. Joshi, S.S.; Dhoble, A.S. Photovoltaic-Thermal systems (PVT): Technology review and future trends. *Renew. Sustain. Energy Rev.* **2018**, *92*, 848–882. [CrossRef]
30. Al-Waeli, A.H.; Sopian, K.; Kazem, H.A.; Chaichan, M.T. Photovoltaic/Thermal (PV/T) systems: Status and future prospects. *Renew. Sustain. Energy Rev.* **2017**, *77*, 109–130. [CrossRef]
31. Ho, C.J.; Chou, W.L.; Lai, C.M. Thermal and electrical performance of a water-surface floating PV integrated with a water-saturated MEPCM layer. *Energy Convers. Manag.* **2015**, *89*, 862–872. [CrossRef]

32. Nižetić, S.; Čoko, D.; Yadav, A.; Grubišić-Čabo, F. Water spray cooling technique applied on a photovoltaic panel: The performance response. *Energy Convers. Manag.* **2016**, *108*, 287–296. [CrossRef]
33. Alami, A.H. Effects of evaporative cooling on efficiency of photovoltaic modules. *Energy Convers. Manag.* **2014**, *77*, 668–679. [CrossRef]
34. Alizadeh, H.; Nazari, M.A.; Ghasempour, R.; Shafii, M.B.; Akbarzadeh, A. Numerical analysis of photovoltaic solar panel cooling by a flat plate closed-loop pulsating heat pipe. *Sol. Energy* **2020**, *206*, 455–463. [CrossRef]
35. Smith, C.J.; Forster, P.M.; Crook, R. Global analysis of photovoltaic energy output enhanced by phase change material cooling. *Appl. Energy* **2014**, *126*, 21–28. [CrossRef]
36. Chander, S.; Purohit, A.; Sharma, A.; Nehra, S.P.; Dhaka, M.S. Impact of temperature on performance of series and parallel connected mono-crystalline silicon solar cells. *Energy Rep.* **2015**, *1*, 175–180. [CrossRef]
37. Charalambous, P.G.; Maidment, G.G.; Kalogirou, S.A.; Yiakoumetti, K. Photovoltaic thermal (PV/T) collectors: A review. *Appl. Therm. Eng.* **2007**, *27*, 275–286. [CrossRef]
38. Wu, J.; Zhang, X.; Shen, J.; Wu, Y.; Connelly, K.; Yang, T.; Wang, H. A review of thermal absorbers and their integration methods for the combined solar photovoltaic/thermal (PV/T) modules. *Renew. Sustain. Energy Rev.* **2017**, *75*, 839–854. [CrossRef]
39. Srithar, K.; Akash, K.; Nambi, R.; Vivar, M.; Saravanan, R. Enhancing photovoltaic efficiency through evaporative cooling and a solar still. *Sol. Energy* **2023**, *265*, 112134. [CrossRef]
40. Elbreki, A.M.; Sopian, K.; Fazlizan, A.; Ibrahim, A. An innovative technique of passive cooling PV module using lapping fins and planner reflector. *Case Stud. Therm. Eng.* **2020**, *19*, 100607. [CrossRef]
41. Mahmood, D.M.; Aljubury, I.M.A. Experimental investigation of a hybrid photovoltaic evaporative cooling (PV/EC) system performance under arid conditions. *Results Eng.* **2022**, *15*, 100618. [CrossRef]
42. Hasan, H.A.; Sherza, J.S.; Mahdi, J.M.; Togun, H.; Abed, A.M.; Ibrahim, R.K.; Yaïci, W. Experimental evaluation of the thermoelectrical performance of photovoltaic-thermal systems with a water-cooled heat sink. *Sustainability* **2022**, *14*, 10231. [CrossRef]
43. Aamir Al-Mabsali, S.; Candido, J.P.; Chaudhry, H.N.; Gul, M.S. Investigation of an inclined heat pipe heat exchanger as a passive cooling mechanism on a photovoltaic panel. *Energies* **2021**, *14*, 7828. [CrossRef]
44. Sukamongkol, Y.; Chungpaibulpatana, S.; Limmeechokchai, B.; Sripadungtham, P. A Simulation Model for Predicting the Transient Performance of a Hybrid PV/T Forced-Circulation Solar Water-Heating System. In Proceedings of the 8th World Renewable Energy Congress (WREC VIII), Denver, CO, USA, 28 August–3 September 2004.
45. Pérez Grajales, S. Simulation and Characterization of an Advanced Solar-Thermal-Photovoltaic Hybrid System. Ph.D. Thesis, UAEM, Cuernavaca, Mexico, 2019.
46. Manrique, J.A. *Energía Solar: Fundamentos y Aplicaciones Fototérmicas*; No. 621.47 M3; Ed. Harla: Mexico City, Mexico, 1984.
47. Gasquet, H.L. *Conversión de la Luz Solar en Energía Eléctrica—Manual Teórico Practico*; Gasquet: Mexico City, Mexico, 2004; Volume 4, pp. 17–32.
48. Singh, P.; Ravindra, N.M. Analysis of series and shunt resistance in silicon solar cells using single and double exponential models. *Emerg. Mater. Res.* **2012**, *1*, 33–38. [CrossRef]
49. *NOM 003-ENER-2011*; Thermal Efficiency of Water Heaters for Domestic and Commercial Use, (Limits, Test Methods, and Labeling that Provide a Methodology for Calculating the Solar System). Universidad Autónoma Metropolitana-Azcapotzalco, Revista Del Desarrollo Tecnológico: Azcapotzalco, Mexico, 2018; pp. 2–7, 27–33.
50. Ashrae, A. *ASHRAE 93-1986*; Method of Testing to Determine the Thermal Performance of Solar Collectors. American Society of Heating. Refrigerating and Air-Conditioning Engineers, Inc.: Atlanta, GA, USA, 1986.
51. Coleman, H.W.; Steele, W.G. *Experimentation, Validation, and Uncertainty Analysis for Engineers*; John Wiley & Sons: Hoboken, NJ, USA, 2018.